Anharmonic line shift and linewidth of the Raman mode in covalent semiconductors

G. Lang
Institut für Theoretische Physik, Universität Regensburg, D-93040 Regensburg, Germany

K. Karch
Institut für Festkörpertheorie and Theoretische Optik, Universität Jena, D-07743 Jena, Germany

M. Schmitt and P. Pavone
Institut für Theoretische Physik, Universität Regensburg, D-93040 Regensburg, Germany

A. P. Mayer
Max-Planck-Institut für Physik komplexer Systeme, D-01187 Dresden, Germany

R. K. Wehner
Institut für Theoretische Festkörperphysik, Universität Münster, D-48149 Münster, Germany

D. Strauch
Institut für Theoretische Physik, Universität Regensburg, D-93040 Regensburg, Germany
(Received 15 September 1998)

Combining density-functional perturbation theory with the frozen-phonon approach, the anharmonic shift of the Raman frequency of the covalent semiconductors diamond and silicon are determined *ab initio*. The temperature dependence of the Raman frequency and the contribution of zero-point motion are calculated as well as the Raman linewidth. Corresponding results for germanium have been obtained with the assumption that the quartic anharmonic force constants may be approximated by those of silicon. [S0163-1829(99)13305-8]

I. INTRODUCTION

Due to a large number of available experimental data and numerous models as well as *ab initio* calculations of phonon frequencies and eigenvectors, lattice-dynamical effects in the covalent elemental semiconductors diamond, silicon, and germanium, which may be treated in the harmonic approximation, are nowadays quite well understood. However, there are important phenomena that result from the anharmonicity of the lattice potential. These are much more difficult to describe in the framework of model calculations because of the large number of parameters involved in anharmonic extensions of lattice-dynamical models. Here, *ab initio* techniques based on density-functional theory, which have been very successful in applications to semiconductors (for a recent review see Ref. 1), have led to a breakthrough for a quantitative description of anharmonic properties free of fitting parameters. Such calculations are needed for various reasons. They help to achieve a more detailed understanding of anharmonic processes in crystals and allow for predictions of material properties. Furthermore, they serve to assess the quality of lattice-dynamical calculations based on the harmonic approximation, as they quantify the difference between harmonic quantities and the corresponding physical quantities measured in experiments, which contain anharmonic contributions.

The physical properties focused on in this paper are the intrinsic linewidth and anharmonic frequency shift of the triply degenerate zone-center optical mode of the covalent semiconductors, which have been studied extensively by Raman scattering as functions of temperature[2–14] (for detailed discussions of the experimental work see Refs. 13 and 14; recent experimental data on the Raman frequency and linewidth of diamond for various isotopic compositions can be found in Refs. 15–18, data on the linewidth of germanium for various isotopic compositions in Ref. 19). Since the vibrational amplitudes of the atoms due to thermal and zero-point motion are small in these materials for temperatures at and below room temperature, one may use perturbation theory involving low-order anharmonicity only. Since the early work of Cowley[20] and Klemens,[21] there has been a number of attempts to calculate phonon lifetimes and partly anharmonic frequency shifts of elemental semiconductors in the framework of anharmonic lattice-dynamical models.[22–24] To overcome the problem of insufficient experimental data to fit the parameters of an anharmonic lattice-dynamical model, Narasimhan and Vanderbilt[25] have determined certain cubic anharmonic coupling constants by *ab initio* frozen phonon calculations and fitted to these a Keating model.[26] In this way, they calculated both the Raman linewidth and anharmonic frequency shift for silicon, the latter, however, without the contribution of quartic anharmonicity. A different approach to determine theoretically the temperature dependence of the Raman frequency and linewidth had been chosen by Wang *et al.*[27] They performed molecular dynamics simulations on the basis of a semiempirical tight-binding ansatz for the crystal energy. This technique is well suited for high temperatures, since it accounts, in principle, for an-

harmonicity of any order. However, treating the atomic motion classically, it cannot deal properly with the low-temperature quantum regime. In a pioneering work,[28] Debernardi *et al.* have performed the first truly *ab initio* calculations of Raman linewidths for semiconductor crystals. A calculation of this quantity within perturbation theory of lowest order requires cubic anharmonicity only. The authors of Ref. 28 have determined the cubic anharmonic coupling constants by extending density-functional perturbation theory (DFPT) using the $(2n+1)$ theorem.[29] For a calculation of the anharmonic shift of the Raman frequency in perturbation theory, quartic anharmonicity enters at the same order of $\hbar$ as the cubic one. A determination of the corresponding quartic anharmonic coupling constants via the $(2n+1)$ theorem is complicated by the fact that unlike the case of cubic anharmonicity, the linear response of the Kohn-Sham wave functions to phonon mode displacements is no longer sufficient. We therefore proceed in a different way, combining density-functional perturbation theory and the frozen-phonon approach and making use of the high symmetry of the Raman modes. The cubic (quartic) anharmonic coupling constants needed for the calculation of the linewidth and anharmonic frequency shift are determined by differentiating once (twice) numerically with respect to the amplitude of the Raman mode dynamical matrices that have been calculated using DFPT. In this way, the anharmonic shift of the Raman frequency has been calculated for fully *ab initio*. First results for diamond with yet limited accuracy had been presented in Ref. 30. Here, we present and discuss results for diamond and silicon. In the case of germanium, we have determined the cubic anharmonic coupling constants via the $(2n+1)$ theorem, while for the quartic anharmonic force constants the corresponding values of silicon have been used. Since the contribution of quartic anharmonicity to the anharmonic frequency shift was found to be considerably smaller than that of the cubic one, this approximation (termed the mass approximation in other contexts) should be acceptable for an estimate of the anharmonic line shift.

In the following section, our approach is described in some detail. Section III contains some technical details of our numerical calculations based on density-functional theory and the local density approximation. In Sec. IV, results are presented for the Raman linewidth of C, Si, and Ge. They are compared with experimental and other theoretical data available from the literature. Section V is then concerned with the anharmonic shift of the Raman frequency. Specifically, results on the temperature dependence of the Raman frequency are presented and quantitative predictions are made for the deviation of the $1/\sqrt{M}$ dependence of the Raman frequency on isotope mass M. The paper concludes with a final discussion.

II. GENERAL THEORY

In the framework of interacting phonon theory,[31] the intrinsic linewidth $\overline{\Gamma}_{\mathbf{q}j}$ and the anharmonic frequency shift $\Delta_{\mathbf{q}j}$ of a phonon mode with wave vector $\mathbf{q}$ and belonging to branch j of a weakly anharmonic crystal follows from the frequency-dependent retarded self-energy $\Pi_{\mathbf{q}j}(\omega)$ of this mode:

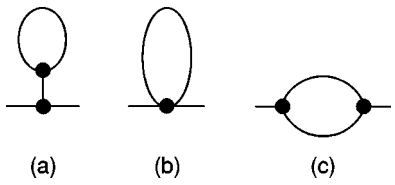

FIG. 1. Diagrammatic representation of the leading anharmonic contributions in perturbation theory to the Raman frequency: (a) tadpole diagram, (b) loop diagram, and (c) bubble diagram.

$$\Pi_{\mathbf{q}j}(\omega_{\mathbf{q}j}) = \Delta_{\mathbf{q}j} - i\overline{\Gamma}_{\mathbf{q}j}, \tag{2.1}$$

where $\omega_{\mathbf{q}j}$ may be taken as the harmonic frequency of the phonon mode $(\mathbf{q}j)$. Lowest-order perturbation theory yields the well-known three contributions to the self-energy which are symbolized by the three diagrams of Fig. 1 and which, in the limit of zero temperature, are the lowest-order (first-order) terms in an expansion of the self-energy in powers of $\hbar$. When specialized to a Raman mode $(\mathbf{q}=\mathbf{0}, j=R)$, the corresponding expressions are explicitly

$$\Pi_{\mathbf{0}R}(\omega) = \Pi_{\mathbf{0}R}^{(T)} + \Pi_{\mathbf{0}R}^{(L)} + \Pi_{\mathbf{0}R}^{(B)}(\omega), \tag{2.2}$$

where

$$\Pi_{\mathbf{0}R}^{(T)} = \sum_{\alpha,\beta} V_{3,\alpha\beta}(\mathbf{0}R, \mathbf{0}R, -)\,\eta_{\alpha\beta}, \tag{2.3a}$$

$$\Pi_{\mathbf{0}R}^{(L)} = \frac{1}{2}\sum_{\mathbf{q}j} V_4(\mathbf{0}R, \mathbf{0}R, \mathbf{q}j, -\mathbf{q}j)(2n_{\mathbf{q}j}+1), \tag{2.3b}$$

$$\Pi_{\mathbf{0}R}^{(B)}(\omega) = -\frac{1}{2}\sum_{\mathbf{q}j,j'} |V_3(\mathbf{0}R, \mathbf{q}j, -\mathbf{q}j')|^2 \times \left\{ \frac{2(\omega_{\mathbf{q}j}+\omega_{\mathbf{q}j'})}{(\omega_{\mathbf{q}j}+\omega_{\mathbf{q}j'})^2-(\omega+i\varepsilon)^2}(1+n_{\mathbf{q}j}+n_{\mathbf{q}j'}) + \frac{2(\omega_{\mathbf{q}j}-\omega_{\mathbf{q}j'})}{(\omega_{\mathbf{q}j}-\omega_{\mathbf{q}j'})^2-(\omega+i\varepsilon)^2}(n_{\mathbf{q}j'}-n_{\mathbf{q}j}) \right\}. \tag{2.3c}$$

Here, $n_{\mathbf{q}j}$ is the Bose factor $[\exp(\hbar\omega_{\mathbf{q}j}/K_BT)-1]^{-1}$. The cubic (V_3) and quartic (V_4) coupling coefficients occur in an expansion of the lattice potential energy U around the classical equilibrium positions of the atoms in powers of phonon normal coordinates $A(\mathbf{q}j) = a_{\mathbf{q}j} + a_{-\mathbf{q}j}^{\dagger}$, where $a^{\dagger}$ and a are phonon creation and annihilation operators, and in powers of the components of the Lagrangian strain tensor $(\eta_{\alpha\beta})$

$$V_n(\mathbf{q}_1 j_1, \mathbf{q}_2 j_2, \ldots) = \frac{1}{\hbar}\frac{\partial^n}{\partial A(\mathbf{q}_1 j_1)\partial A(\mathbf{q}_2 j_2)\cdots}U, \tag{2.4a}$$

$$V_{3,\alpha\beta}(\mathbf{q}j, \mathbf{q}'j', -) = \frac{1}{\hbar}\frac{\partial^3}{\partial A(\mathbf{q}j)\partial A(\mathbf{q}'j')\partial\eta_{\alpha\beta}}U. \tag{2.4b}$$

The derivatives in Eq. (2.4) have to be taken at the classical equilibrium configuration of the crystal.

For cubic crystals, the first (tadpole) contribution to the self-energy may be expressed in the simple form

$$\Pi^{(T)}_{\mathbf{0}R} = -3\,\omega_{\mathbf{0}R}\,\gamma(\mathbf{0}R)\,\frac{\Delta a}{a}, \tag{2.5}$$

where $\gamma(\mathbf{0}R)$ is the Grüneisen constant of the Raman mode and $\Delta a/a$ is the relative change of the lattice constant due to zero-point and thermal motion of the atoms. First-order perturbation theory yields the well-known expression

$$\frac{\Delta a}{a} = \frac{\hbar}{6B_0V}\sum_{\mathbf{q}j}\ \omega_{\mathbf{q}j}\,\gamma(\mathbf{q}j)(2n_{\mathbf{q}j}+1), \tag{2.6}$$

where B_0 is the bulk modulus and V the crystal volume. *Ab initio* calculations of the mode Grüneisen constants $\gamma(\mathbf{q}j)$ had been carried out earlier for diamond, silicon, and germanium by differentiating numerically the phonon frequencies with respect to the lattice constant a at its equilibrium value.[32,33] We note that $\Pi^{(T)}_{\mathbf{0}R}$ can be determined from experimental data alone. The Grüneisen constants of the Raman mode have been determined by Raman scattering for diamond,[34] silicon,[35] and germanium.[36] The relative change in lattice constant may be calculated from

$$\frac{\Delta a(T)}{a} = \frac{\Delta a(0)}{a} + \int_0^T \alpha(T')dT', \tag{2.7}$$

where $\alpha(T)$ is the linear thermal expansion coefficient. The relative shift $\Delta a(0)/a$ of the lattice constant due to zero-point motion can be determined by a linear extrapolation down to $T=0$ from the regime, where $\Delta a(T)/a$ is linear in T. This may be very inaccurate as the linear regime may be unrecognizably small. Another way involves the isotope effect on the lattice constant. If a_1 is the lattice constant at $T=0$ for a crystal made of one isotope with mass M_1 and a_2 is the lattice constant of a crystal with isotope mass M_2, Eq. (2.6) implies that

$$\frac{\Delta a_1(0)}{a_1} = \frac{a_1(0)-a_2(0)}{a_1(1-\sqrt{M_1/M_2})}. \tag{2.8}$$

By determining $\Pi^{(T)}_{\mathbf{0}R}$ in this way, one obtains already an order of magnitude estimate of the effect of anharmonicity on the Raman frequency.

In order to evaluate the bubble and the loop diagrams of Fig. 1, the anharmonic coupling constants $V_3(\mathbf{0}R,\mathbf{q}j,-\mathbf{q}j')$ and $V_4(\mathbf{0}R,\mathbf{0}R,\mathbf{q}j,-\mathbf{q}j)$ have to be known for a grid of wave vectors $\mathbf{q}$ in the first Brillouin zone. To determine them, we calculate dynamical matrices for the crystal lattice in its classical equilibrium configuration as well as for a crystal structure with a displacement pattern of the form

$$u_\alpha(l\kappa) = \varepsilon\,(a/2)\,(-1)^\kappa \tag{2.9}$$

frozen in, where l labels the unit cells and $\kappa=1,2$ the two sublattices in the diamond structure. We denote these dynamical matrices by $\mathbf{D}^{(\varepsilon)}$ and adopt the definition

$$D^{(\varepsilon)}_{\alpha\beta}(\kappa\kappa'|\mathbf{q}) = \frac{1}{M}\sum_l\ \Phi^{(\varepsilon)}_{\alpha\beta}(0\kappa,l\kappa')e^{i\mathbf{q}\cdot\mathbf{R}(l)}. \tag{2.10}$$

Here $\mathbf{R}(l)$ is the position vector of the unit cell l, while α,β are Cartesian indices, and $\Phi^{(\varepsilon)}_{\alpha\beta}(l\kappa,l'\kappa')$ are the harmonic force constants of the crystal in a static nonequilibrium configuration with the optic displacement pattern of amplitude ε frozen in. The desired cubic and quartic anharmonic coupling constants are then obtained as derivatives of the dynamical matrices with respect to ε, namely,

$$V_3(\mathbf{0}R,\mathbf{q}j,-\mathbf{q}j') = \sqrt{\frac{\hbar}{12a^2MN\omega_{\mathbf{q}j}\omega_{\mathbf{q}j'}\omega_{\mathbf{0}R}}} \times\sum_{\kappa,\kappa'}\sum_{\alpha,\beta} e_\alpha(\kappa|\mathbf{q}j)e^*_\beta(\kappa'|\mathbf{q}j') \times\left[\frac{\partial}{\partial\varepsilon}D^{(\varepsilon)}_{\alpha\beta}(\kappa\kappa'|\mathbf{q})\right]_{\varepsilon=0} \tag{2.11}$$

and likewise

$$V_4(\mathbf{0}R,\mathbf{0}R,\mathbf{q}j,-\mathbf{q}j') = \sqrt{\frac{\hbar^2}{36a^4M^2N^2\omega_{\mathbf{q}j}\omega_{\mathbf{q}j'}\omega^2_{\mathbf{0}R}}} \times\sum_{\kappa,\kappa'}\sum_{\alpha,\beta} e_\alpha(\kappa|\mathbf{q}j)e^*_\beta(\kappa'|\mathbf{q}j') \times\left[\frac{\partial^2}{\partial\varepsilon^2}D^{(\varepsilon)}_{\alpha\beta}(\kappa\kappa'|\mathbf{q})\right]_{\varepsilon=0}, \tag{2.12}$$

where N is the number of unit cells and M the atomic mass. The quantity $e_\alpha(\kappa|\mathbf{q}j)$ is a component of the eigenvector of the dynamical matrix $\mathbf{D}^{(0)}(\mathbf{q})$ associated with branch j.

III. TECHNICAL ASPECTS

In practice, the dynamical matrices $\mathbf{D}(\mathbf{q})$ are determined on a uniform grid of eight $\mathbf{q}$ points in the irreducible part of the Brillouin zone, as described in Ref. 37. An interpolation scheme has then been used that first transforms the dynamical matrices into real space, producing force constants between up to ninth nearest neighbors. The numerical derivatives with respect to ε have then been carried out in real space rather than in Fourier space. From these derivatives of force constants, the quantities $\partial^n\mathbf{D}(\mathbf{q})/\partial\varepsilon^n$ have then been calculated via a Fourier transform on $\mathbf{q}$ grids of desired form and density. To obtain numerical derivatives with sufficient accuracy, dynamical matrices have been computed for 11 different values of ε ranging from -0.02 to $+0.02$. From the dynamical matrices at $\varepsilon=0$, the frequencies and eigenvectors of the phonon modes in the equilibrium configuration of the crystal have been determined.

The dynamical matrices have been calculated within density-functional perturbation theory on the basis of the local density approximation. For the correlation potential, the parametrization of Perdew and Zunger[38] of the Monte Carlo data of Ceperley and Alder[39] has been used. The Kohn-Sham wave functions are expanded in plane-wave basis sets with the kinetic energy cutoff chosen as 60 Ry for diamond and 18 Ry for silicon. Soft norm-conserving pseudopotentials have been constructed for C and Si using the method of Troullier and Martins.[40] The variation of the cubic and quartic anharmonic coupling coefficients $\sqrt{N}V_3(\mathbf{0}R,\mathbf{q}j,-\mathbf{q}j)$ and

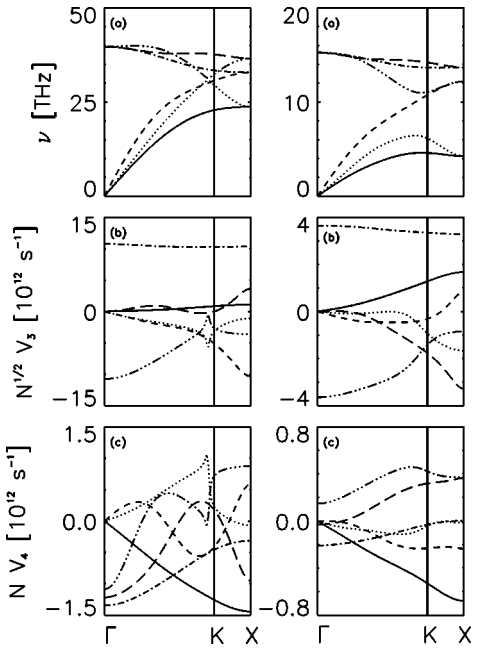

FIG. 2. Phonon dispersion curves (a) and cubic (b) and quartic (c) anharmonic coupling constants as functions of wave vector along the Σ direction (1,1,0) for diamond (left) and silicon (right). The eigenvector of the Raman mode is along the (1,1,1) direction $[e_\alpha(2|\mathbf{0}R)=1/\sqrt{6}]$.

$NV_4(\mathbf{0}R,\mathbf{0}R,\mathbf{q}j,-\mathbf{q}j)$ as a function of $\mathbf{q}$ along the (1,1,0) direction is shown in Fig. 2. An interesting feature is the strong variation of some cubic and quartic coupling coefficients of diamond in the neighborhood of the K point which is associated with an avoided crossing of two branches in the frequency dispersion relation. In Table I, values for cubic anharmonic force constants of silicon as defined in Ref. 41 are compared with the results of two other *ab initio* approaches. One of them uses DFPT and the $(2n+1)$ theorem, while the second one is a frozen-phonon calculation. The agreement is quite satisfactory in view of the technical differences in the calculations concerning, e.g., the kinetic energy cutoffs and the sums over the electronic eigenstates in the Brillouin zone. Also shown in Table I are values for cubic anharmonic force constants resulting from a nonlinear lattice-dynamical model that combines the shell model with the bond charge model.[23,42] Apart from various optical and harmonic lattice-dynamical quantities, the model parameters had been fitted to elements of mode Grüneisen tensors, i.e., to quantities characterizing the interaction of acoustic zone-center modes with other phonon modes. The force constants in Table I describe the anharmonic coupling between the optical zone-center modes and phonon modes of the X point at the Brillouin zone boundary. While the model results for four of the six force constants are in very good agreement with the *ab initio* data, the quantities $I_{z\overline{bb}}$ and $I_{\overline{ybc}}$ deviate noticeably.

TABLE I. Cubic anharmonic force constants for Si and Ge as defined in Ref. 41 in units of eV/Å^3.

	B_{xyz}	$I_{z\overline{aa}}$	$I_{z\overline{bb}}$	$I_{z\overline{cc}}$	$I_{\overline{xac}}$	$I_{\overline{ybc}}$
DM[a]	−289.75	233.85	−36.10	53.35	452.25	−63.64
DFPT[b]	−285.96	226.90	−37.65	49.41	441.80	−63.16
FP[c]	−290.4	315.20	−49.12	46.48		
SBCM[d]	−306.0	232.0	7.0	50.0	452.0	−100.0
DFPT[e]	−233.71	194.94	−34.95	44.43	365.49	−58.61

[a]Si, numerical derivatives of dynamical matrices (this work).
[b]Si, density-functional perturbation theory (Ref. 43)
[c]Si, frozen-phonon calculations (Ref. 41)
[d]Si, nonlinear shell-bond-charge model (Refs. 23,42).
[e]Ge, density-functional perturbation theory (this work).

In the case of germanium, the cubic anharmonic force constants have been calculated using DFPT and the $(2n+1)$ theorem in the same way as in Ref. 28. The pseudopotential for germanium has been constructed following a scheme suggested by von Barth and Car,[44] and the kinetic energy cutoff was 24 Ry. For the quartic anharmonic force constants in the calculation of the V_4 coefficients for germanium, we have used the corresponding values for silicon determined in the way described above. This ''mass approximation'' should be justified here in view of the fact that the loop diagram yields the smallest contribution to the self-energy. To assess to some extent the quality of this approximation, we compare in Table I cubic anharmonic force constants of germanium determined by DFPT with those of silicon. It is found that the mass approximation yields values having a modulus consistently too large. However, the discrepancies are less than 24% in the worst cases. We may expect a similar situation with the V_4 coefficients.

For the evaluation of the bubble diagram, we have first calculated the damping function $\Gamma_{\mathbf{0}R}(\omega)=-\operatorname{Im}\Pi_{\mathbf{0}R}(\omega)$, which has the explicit form

$$\Gamma_{\mathbf{0}R}(\omega)=\frac{\pi}{2}\sum_{\mathbf{q},j,j'}|V_3(\mathbf{0}R,\mathbf{q}j,-\mathbf{q}j')|^2\{[1+n_{\mathbf{q}j}+n_{\mathbf{q}j'}]\times\delta(\omega_{\mathbf{q}j}+\omega_{\mathbf{q}j'}-\omega)+2[n_{\mathbf{q}j'}-n_{\mathbf{q}j}]\times\delta(\omega_{\mathbf{q}j}-\omega_{\mathbf{q}j'}-\omega)\}. \tag{3.1}$$

This function has been determined by a sampling procedure that divides the frequency range between zero and twice the maximal phonon frequency into 400 channels of equal size. Phonon frequencies and V_3 coefficients have been provided on a coarse grid of 916 $\mathbf{q}$ vectors in an irreducible segment of the Brillouin zone. By quadratic interpolation of the phonon frequencies, a finer grid of up to $9^3\times916$ wave vectors was generated. The results have been tested against variations of the grid size and are shown in Fig. 3 for temperature $T=0$ K.

Since the static optic displacement vector (2.9) is not invariant under all point group operations of the diamond structure, the summations over wave vectors $\mathbf{q}$ have to be extended over four nonequivalent irreducible segments of the Brillouin zone.

The real part of the self-energy at frequency $\omega_{\mathbf{0}R}$ has been obtained from the damping function $\Gamma_{\mathbf{0}R}(\omega)$ via Kramers-Kronig transformation.

For the evaluations of the loop diagram and the tadpole diagram, grids of special points[45] have been used that correspond to 182 $\mathbf{q}$ vectors in an irreducible segment of the Brillouin zone.

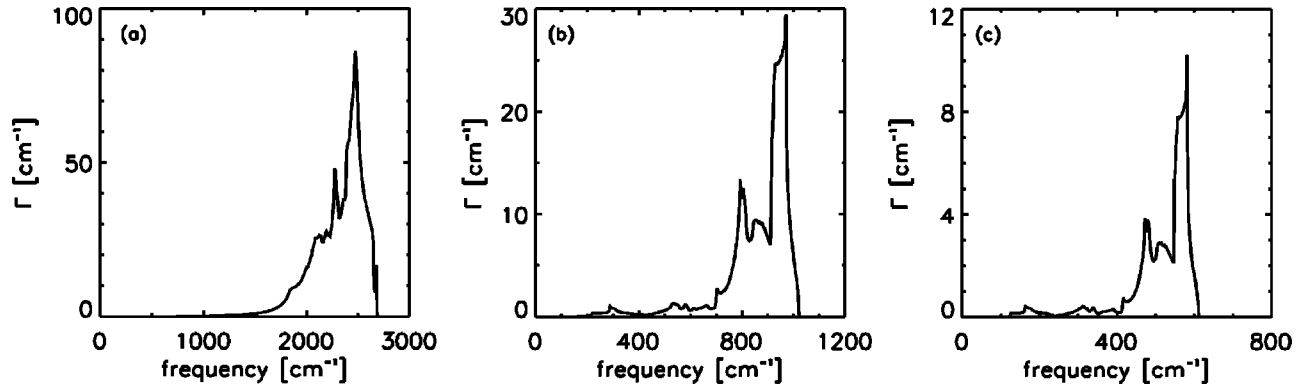

FIG. 3. Damping functions $\Gamma_{0R}(\omega)$ for C (a), Si (b), and Ge (c).

IV. INTRINSIC LINE WIDTH

In a perfect weakly anharmonic crystal, the shape of the Raman lines is a Lorentzian to a good approximation with the full width at half maximum (FWHM) being equal to $2\overline{\Gamma}_{0R}$. *Ab initio* calculations of this quantity had been performed earlier by Debernardi *et al.*,[28] and our data are in good agreement with their earlier calculations. The widths due to spontaneous decay at zero temperature have been found to be 0.97 cm^{-1} for C, 1.44 cm^{-1} for Si, and 0.69 cm^{-1} for Ge, while the corresponding values of Ref. 28 are 1.01 cm^{-1}, 1.48 cm^{-1}, and 0.67 cm^{-1}, respectively.

In Fig. 4, our results for the temperature dependence of the Raman linewidth of diamond, silicon, and germanium are compared with experimental data. Except for diamond, where the experimental data show a large scatter and are consistently larger than the theoretical ones, the agreement between theory and experiment is quite satisfactory.

V. ANHARMONIC LINE SHIFT

The real part of the self-energy Π_{0R} gives rise to a shift of the Raman frequency to which all three diagrams of Fig. 1 contribute. Unlike the situation of the anharmonic corrections to the bulk moduli of C and Si,[47] where strong compensations occur between the three different terms imposing high requirements on the numerical accuracy of these terms, all three contributions to the Raman frequency are negative for the three materials (Fig. 5). While the contributions of the tadpole diagram and the bubble diagram are approximately of the same order of magnitude at low temperatures, the loop diagram is found to yield a contribution much smaller than the other two. Only at high temperatures in the case of silicon does the loop diagram reach the same magnitude as the tadpole diagram, but is much smaller than the contribution of the bubble diagram. In the case of germanium, the loop diagram has been evaluated with the quartic anharmonic coupling constants of silicon. Assuming that the relative error in the quartic anharmonic constants due to this mass approximation is not larger than that for the cubic ones (Table I), and considering the smallness of the contribution of the loop diagram to the anharmonic frequency shift, we estimate that the error of the latter quantity due to the mass approximation should be less than 1.5% at $T=0$ K and less than 7% at room temperature.

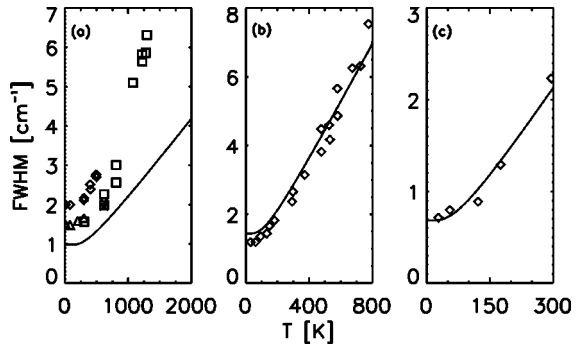

FIG. 4. Raman linewidths. (a) diamond. Experimental data from Ref. 14 (rectangular symbols), Ref. 6 (diamonds), Ref. 5 (triangles). (b) Si and (c) Ge. Experimental data from Ref. 13 (diamonds).

To obtain the physical frequency as measured from the position of the Raman line, one has to add the contributions of the three self-energy diagrams of Fig. 1 to the bare (harmonic) Raman frequency. However, the latter is only known with an accuracy that is smaller than the size of the anharmonic contributions, as may be seen from Table II. Here, our harmonic Raman frequencies $\nu_{harmonic}$ are compared with earlier DFPT calculations[32,37] and experimental values $\nu_{experimental}$. The anharmonic shifts $\Delta\nu$ at zero temperature are also displayed. Obviously, the harmonic frequencies are consistently too low for the equation $\nu_{experimental} = \nu_{harmonic} + \Delta\nu$ to be satisfied. This may be a deficiency of the local density approximation. To compare our results on the temperature dependence of the Raman frequency with experimental data, we have therefore shifted our data to the experimental value at $T=0$ in Fig. 5. In the case of diamond at temperatures below 500 K, the temperature dependence agrees well with the experimental data of Anastassakis *et al.*,[6] whereas at elevated temperatures, the slope appears to agree slightly better with those of Herchen and Capelli.[14] In the case of silicon, very good agreement is found with the experimental data of Menéndez and Cardona[13] as well as with the data by Tsu and Hernandez,[11] the latter measured at and above room temperature. For Ge, the agreement is not as good as for silicon. The discrepancy may be partly due to the error in the calculations introduced by the mass approximation for the quartic anharmonic coupling constants.

The theoretical data in Table II (the harmonic frequency $\nu_{harmonic}$ and the anharmonic frequency shift $\Delta\nu$) refer to the

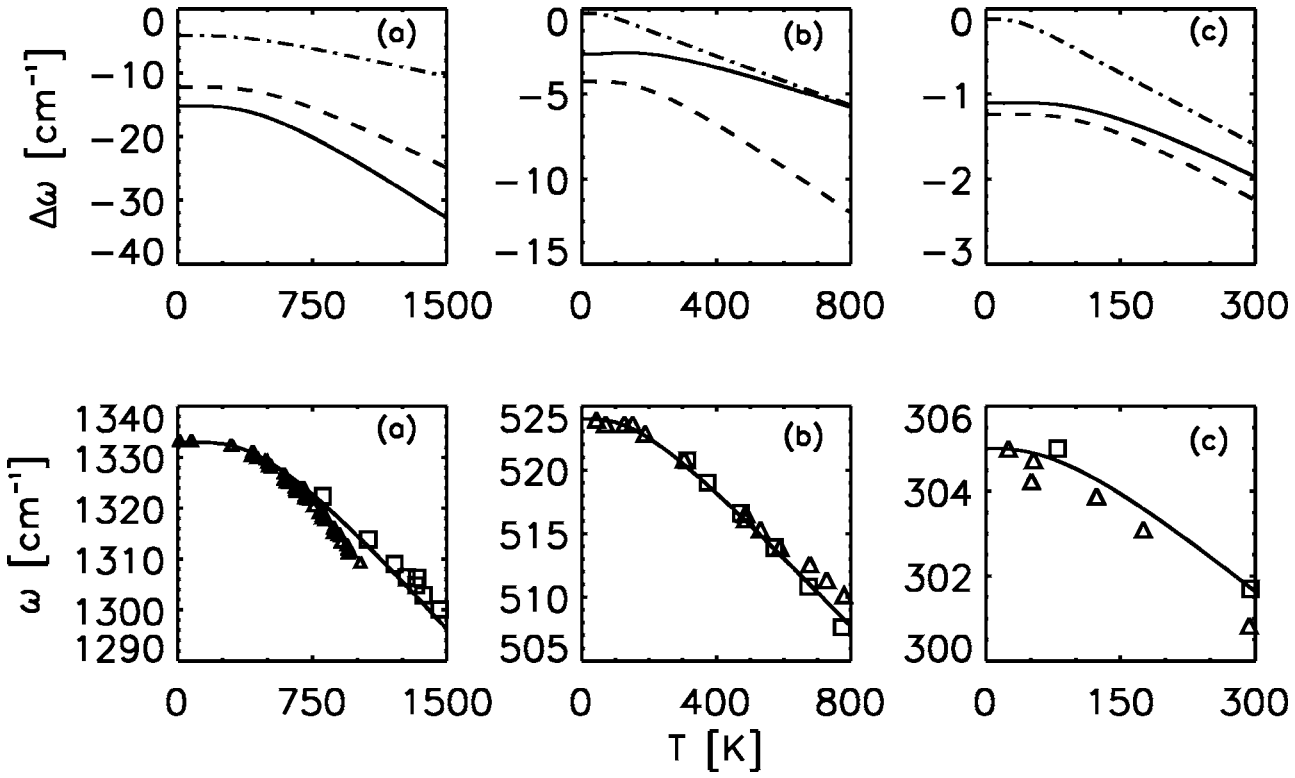

FIG. 5. Upper panel: contributions of the three diagrams of Fig. 1 to the anharmonic shift $\Delta\nu$ of the Raman frequency of C (a), Si (b), and Ge (c). Solid line, tadpole diagram; dashed line, bubble diagram; dash-dotted line, loop diagram. Lower panel: temperature dependence of the Raman frequency of C (a), Si (b), and Ge (c). The theoretical data (solid curves) have been shifted to the experimental value of the Raman frequency at $T=0$ K. Experimental data in (a) from Ref. 6 (triangles) and from Ref. 14 (squares). Experimental data in (b) from Ref. 13 (triangles) and from Ref. 11 (squares). Experimental data in (c) from Ref. 13 (triangles) and from Ref. 46 (squares).

natural isotopic composition of the three materials; i.e., in the spirit of the virtual crystal approximation, they have been calculated with a mass M that is an average over the isotope masses weighted with their relative natural abundances. To determine the Raman frequency at $T=0$ K of a crystal consisting of an isotope with mass M_0, one may use the formula

$$\nu(M_0)=\nu_{harmonic}(M)\sqrt{\frac{M}{M_0}}+\Delta\nu(M)\frac{M}{M_0}, \qquad (5.1)$$

which is correct up to first order in $\hbar$. Using this formula, we find for the difference between the Raman frequencies of ^{12}C and ^{13}C a value of 49.9 cm^{-1}, where the second term on the right-hand side of Eq. (5.1) contributes -2.4 cm^{-1}. The Raman scattering results of Vogelgesang *et al.*[18] suggest a value of 51.8 cm^{-1} for the frequency difference.

TABLE II. Raman frequencies of C, Si, and Ge: harmonic values, experimental values at $T=0$, and anharmonic shift $\Delta\nu$ at $T=0$. Unit: cm^{-1}.

	C	Si	Ge
Harmonic[a]	1322	508	304
Harmonic	1324[b]	517[c]	306[c]
Experimental	1333.5[d]	524[e]	305[e]
$\Delta\nu$[a]	−31.6	−7.1	−2.5

[a]This work.
[b]Reference 32.
[c]Reference 37.
[d]Reference 6.
[e]Reference 13.

VI. CONCLUSIONS

In summary, the contributions of anharmonicity of the lattice potential to the Raman frequencies of the elemental semiconductors C, Si, and Ge have been calculated *ab initio* using an approach that combines DFPT with the frozen-phonon method in a way analogous to earlier calculations of the contribution of zero-point and thermal motion to the bulk modulus of diamond.[47] Specifically, we have determined the temperature dependence of the Raman frequency and made predictions concerning $1/M$ corrections to the isotope effect of the Raman frequency. These corrections should be resolvable by modern high-resolution light-scattering techniques. The approach we have chosen relies on the high symmetry of the phonon eigenvector of the Raman mode. Introducing supercells, a calculation of the anharmonic correction of zone-boundary modes should still be feasible. Knowledge of anharmonic corrections to optic phonon frequencies in diamond has become particularly desirable in connection with the problem of overbending of the LO branch in this material.[48,49] Specifically, there does not seem to exist a definite answer to the question of whether the zone-center optic frequency in diamond constitutes a local minimum or rather a saddle point. The anharmonic shift of the Raman frequency is of the same order of magnitude as the overbending found

experimentally.[48,49] If this shift varies as a function of wave vector, it will influence the shape of the LO dispersion curves.

A comparison between our results for the temperature dependence of the Raman frequencies and corresponding experimental data can be made only for temperatures sufficiently low that higher-order phonon processes are still negligible. As found experimentally and reasoned theoretically by Balkanski *et al.*,[12] the Raman frequencies of C and Si show a T^2 dependence at elevated temperatures, which can be described by higher-order self-energy diagrams. An *ab initio* determination of the corresponding vertices occurring in these diagrams seems to be out of reach at the moment. At temperatures sufficiently high such that quantum corrections become unimportant, *ab initio* molecular dynamics methods[50] could be applied to determine the linewidth and frequency of the Raman mode.

ACKNOWLEDGMENTS

Financial support by the Deutsche Forschungsgemeinschaft (Graduiertenkolleg ''Komplexität in Festkörpern: Phononen, Elektronen und Strukturen'') is gratefully acknowledged. We would also like to thank the HLRZ at the KFA Jülich (Project No. K2710000) for granting us Cray computing time.

[1] D. Strauch, P. Pavone, A. P. Mayer, K. Karch, H. Sterner, A. Schmid, Th. Pletl, R. Bauer, and M. Schmitt, in *Festkörperprobleme, Advances in Solid State Physics*, Vol. 37, edited by R. Helbig (Vieweg, Braunschweig, 1997), p. 99.
[2] R. G. N. Nayar, Proc.-Indian Acad. Sci., Sect. A **13**, 284 (1941).
[3] R. S. Krishnan, Proc.-Indian Acad. Sci., Sect. A **24**, 45 (1946).
[4] T. R. Hart, R. L. Aggarwal, and B. Lax, Phys. Rev. B **1**, 638 (1970).
[5] S. A. Solin and A. K. Ramdas, Phys. Rev. B **1**, 1687 (1970).
[6] E. Anastassakis, H. C. Hwang, and C. H. Perry, Phys. Rev. B **4**, 2493 (1971).
[7] W. J. Borer, S. S. Mitra, and K. V. Namjoshi, Solid State Commun. **9**, 1377 (1991).
[8] F. Cerdeira and M. Cardona, Phys. Rev. B **5**, 1440 (1972).
[9] P. A. Temple and C. E. Hathaway, Phys. Rev. B **7**, 3685 (1973).
[10] M. A. Washington and H. Z. Cummins, Phys. Rev. B **15**, 5840 (1977).
[11] R. Tsu and J. G. Hernandez, Appl. Phys. Lett. **41**, 1016 (1982).
[12] M. Balkanski, R. F. Wallis, and E. Haro, Phys. Rev. B **28**, 1928 (1983).
[13] J. Menéndez and M. Cardona, Phys. Rev. B **29**, 2051 (1984).
[14] H. Herchen and M. A. Cappelli, Phys. Rev. B **43**, 11 740 (1991).
[15] R. M. Chrenko, J. Appl. Phys. **63**, 5873 (1988).
[16] K. C. Hass, M. A. Tamor, T. R. Anthony, and W. F. Banholzer, Phys. Rev. B **44**, 12 046 (1991).
[17] J. Spitzer, P. Etchegoin, M. Cardona, T. R. Anthony, and W. F. Banholzer, Solid State Commun. **88**, 509 (1993).
[18] R. Vogelgesang, A. K. Ramdas, S. Rodriguez, M. Grimsditch, and T. R. Anthony, Phys. Rev. B **54**, 3989 (1996).
[19] H. D. Fuchs, C. H. Grein, R. I. Devlen, J. Kuhl, and M. Cardona, Phys. Rev. B **44**, 8633 (1991).
[20] R. A. Cowley, J. Phys. (Paris) **26**, 659 (1965).
[21] P. G. Klemens, Phys. Rev. **148**, 845 (1966).
[22] H. Jex, Phys. Status Solidi B **45**, 343 (1971).
[23] R. K. Wehner, M. Labrot, and D. Geschke (unpublished).
[24] E. Haro-Poniatowski, J. L. Escamilla-Reyes, and K. H. Wanser, Phys. Rev. B **53**, 12 121 (1996).
[25] S. Narasimhan and D. Vanderbilt, Phys. Rev. B **43**, 4541 (1991).
[26] P. N. Keating, Phys. Rev. **145**, 637 (1966); **149**, 674 (1966).
[27] C. Z. Wang, C. T. Chan, and K. M. Ho, Phys. Rev. B **42**, 11 276 (1990); **40**, 3390 (1989).
[28] A. Debernardi, S. Baroni, and E. Molinari, Phys. Rev. Lett. **75**, 1819 (1995).
[29] X. Gonze and J.-P. Vigneron, Phys. Rev. B **39**, 13 120 (1989).
[30] K. Karch, A. P. Mayer, T. Dietrich, G. Lang, W. Windl, P. Pavone, D. Strauch, and F. Bechstedt, in *Proceedings of the 23rd International Conference on the Physics of Semiconductors*, edited by M. Scheffler and R. Zimmermann (World Scientific, Singapore, 1996), p. 301.
[31] H. Bilz, D. Strauch, and R. K. Wehner, in *Handbuch der Physik, Bd. XXV/2d: Licht und Materie*, edited by S. Flügge (Springer, Berlin, 1984).
[32] P. Pavone, K. Karch, O. Schütt, W. Windl, D. Strauch, P. Giannozzi, and S. Baroni, Phys. Rev. B **48**, 3156 (1993).
[33] P. Pavone, Ph.D. thesis, SISSA, Trieste, 1991.
[34] H. Boppart, J. van Straaten, and I. F. Silvera, Phys. Rev. B **32**, 1423 (1985), and references therein.
[35] B. A. Weinstein and G. J. Piermarini, Phys. Rev. B **12**, 1172 (1975), and references therein.
[36] C. J. Buchenauer, F. Cerdeira, and M. Cardona, in *Proceedings of the 2nd International Conference on Light Scattering in Solids*, edited by M. Balkanski (Flammarion, Paris, 1971), p. 280.
[37] P. Giannozzi, S. de Gironcoli, P. Pavone, and S. Baroni, Phys. Rev. B **43**, 7231 (1991).
[38] J. P. Perdew and A. Zunger, Phys. Rev. B **23**, 5048 (1981).
[39] D. M. Ceperley and B. J. Adler, Phys. Rev. Lett. **45**, 566 (1980).
[40] N. Troullier and J. L. Martins, Phys. Rev. B **43**, 1993 (1991).
[41] D. Vanderbilt, S. H. Taole, and S. Narasimhan, Phys. Rev. B **40**, 5657 (1989).
[42] M. T. Labrot, A. P. Mayer, and R. K. Wehner, in *Phonons '89*, edited by S. Hunklinger, W. Ludwig, and G. Weiss (World Scientific, Singapore, 1990), Vol. 1, p. 181.
[43] M. Schmitt, Diploma dissertation, Universität Regensburg, 1996.
[44] U. von Barth and R. Car (unpublished).
[45] D. J. Chadi and M. L. Cohen, Phys. Rev. B **8**, 5747 (1973); H. J. Monkhorst and J. D. Pack, *ibid.* **13**, 5188 (1976).
[46] G. Nilsson and G. Nelin, Phys. Rev. B **6**, 3777 (1972).
[47] K. Karch, T. Dietrich, W. Windl, P. Pavone, A. P. Mayer, and D. Strauch, Phys. Rev. B **53**, 7259 (1996).
[48] J. Kulda, B. Dorner, B. Roessli, H. Sterner, R. Bauer, Th. May, K. Karch, P. Pavone, and D. Strauch, Solid State Commun. **99**, 799 (1996).
[49] M. Schwoerer-Böhning, A. T. Macrander, and D. A. Arms, Phys. Rev. Lett. **80**, 5572 (1998).
[50] R. Car and M. Parrinello, Phys. Rev. Lett. **55**, 2471 (1985).